文章编号: 1001-3806(2003)04-0311-06

Nonimaging concentrators in optical wireless communications

Jin Wei, Zhang Haitao, Gong Mali, Yan Ping, Yang Xin, Zhang Kai, Jiang Feng
(Department of Precision Instruments, Tsinghua University, Beijing, 100084)

Abstract: In the field of optical wireless links, concentrators that are designed by the tools of nonimaging optics can be used to collect the light radiation and are more compact and have higher collection efficiencies than imaging concentrators. Hemispherical concentrators are studied by ray tracing, then for several normal nonimaging concentrators: hemispherical concentrators, compound parabolic concentrators (CPC), dielectric totally internally reflecting concentrators (DTIRC), simultaneous multiple surfaces concentrators (SMS) and inhomogeneous media concentrators (Poisson bracket), the design methods and the performances e. g. the gain and the field of view (FOV) are compared as well as the application suggestion.

Key words: nonimaging concentrator; gain; ray tracing; field of view; optical wireless communication

无线光通信中的非成像集中器

金 伟 张海涛 巩马理 闫 平 杨 欣 张 凯 姜 丰
(清华大学精密仪器系数字光电实验室, 北京, 100084)

摘要: 在无线光通信领域, 利用非成像光学设计的集中器能够聚集光辐射能量, 而且相对于成像性集中器具有更紧凑的结构和更高的增益。利用光线追迹法对半球形集中器的性质进行了分析与研究。对好几种非成像集中器: 半球形集中器, 复合抛物线形集中器, 介质内部全反射集中器, 多表面集中器, 多相介质集中器, 从设计原理、增益和视场进行比较, 并分析其应用场合。

关键词: 非成像集中器; 增益; 光线追迹; 视场; 无线光通信
中图分类号: TN929.1 文献标识码: A

Introduction

A wireless optical communication link can have different link configurations. If we adopt the notation such as Table 1, we can summarize six possible link configurations, as illustrated in Fig. 1.

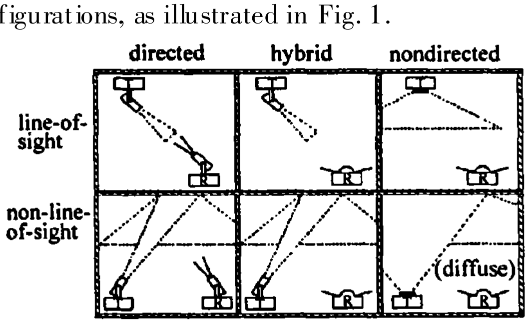

Fig. 1 Configuration for wireless optical links

Table 1 The notation of glossary

glossary	notation
directed	directed transmitter: narrow-beam radiation pattern directed receiver: narrow field of view directed link: consist of a directed transmitter and a directed receiver
non-directed	non-directed transmitter: broad-beam radiation pattern non-directed receiver: wide field of view non-directed link: consist of a directed transmitter and a directed receiver
hybrid	hybrid link: consist of either a directed transmitter and non-directed receiver or non-directed transmitter and a directed receiver
LOS	unobstructed line-of-sight path between the transmitter and receiver
non-LOS	obstructed line-of-sight path between the transmitter and receiver

In the six link configurations, there must be suitable optical devices to collect signal rays. In the optical wireless links, concentrators are used to collect light radiation. The radiation of a source is required

作者简介: 金 伟, 男, 1978 年 1 月出生。硕士。从事无线光通信方面研究工作。

收稿日期: 2003-01-23; 收到修改稿日期: 2003-03-04

to be transferred with as high efficiency as possible onto a given target[1]. The request can be met in the concentrator before a photodiode, which is designed by the tools of nonimaging optics. Nonimaging concentrators may be more compact and have more high collection efficiency than the imaging concentrators.

In this paper, for several normal nonimaging concentrators: hemispherical concentrators, CPC, DTIRC, SMS concentrators and Poisson bracket concentrators, the design methods and the performances e.g. the gain and FOV are compared as well as the application suggestion. In general, hemispherical concentrators have the largest FOV but its gain is the lowest, and the SMS concentrators have the highest gain but its FOV is the smallest. They are applied to diffusing wireless optical indoor communication and directed line-of-sight wireless optical communication respectively.

1 Nonimaging concentrators

According to optical path, the concentrators can be divided into refractive ones, e.g. hemispherical concentrators, refractive-reflective ones, e.g. CPC, DTIRC and SMS concentrator, and variable refractive index concentrator, e.g. Poisson bracket concentrator. They have different design methods and characteristic according to the division.

Signal gain and FOV are two important evaluation indicators. For an ideal, passive three-dimensional concentrator, the thermodynamic-limited signal gain, defined to be the maximum achievable increase of irradiance between the input and the output, is given by[2~4]:

$$C = (N\sin\theta_o/\sin\theta_i)^2 \tag{1}$$

where θ_o and θ_i are the acceptance angles at the output and input apertures respectively, and $N = n_o/n_i$ is the ratio of output and input refractive indices. As the input is generally in the air, i.e., $n_i = 1$, N can be simplified as the refractive index of the concentrator. The angle θ_i is the FOV of the concentrator.

According to different applications, different designs are adopted. In what follows, the design methods and properties of several concentrators are stated.

1.1 Hemispherical concentrator

Hemispherical concentrator as shown in Fig.2 is mainly used in diffusing wireless optical indoor communication system. This concentrator has a half-FOV of 90° and an omnidirectional optical gain of approximately n^2 (n is refractive index)[3,5], as long as its radius is sufficiently large compared to the detector radius.

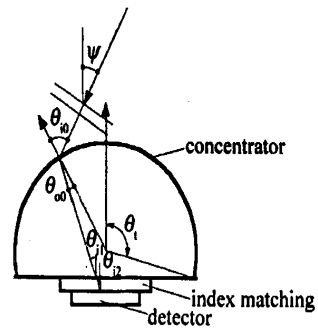

Fig.2 Cross-sectional view of hemispherical concentrator, the angle θ_t is truncated angle

We can study the gain and FOV of the hemisphere concentrator by ray tracing. Supposing a light beam radiates the concentrator uniformly at the angle Ψ (see Fig.2), there are N pieces of rays covering on the concentrator. There are $N_0(\Psi)$ pieces of rays reaching the detector without the concentrator, and there are $N_1(\Psi)$ pieces of rays reaching the detector with the concentrator. Then the gain can be stated:

$$G(\Psi) = N_1(\Psi)/N_0(\Psi) \tag{2}$$

If we defined function:

$$\mathrm{circ}(x, y, r) = \begin{cases} 1 & (x^2 + y^2 \leqslant r^2) \\ 0 & (x^2 + y^2 > r^2) \end{cases} \tag{3}$$

Then $N_0(\Psi)$ and $N_1(\Psi)$ in function(2) may be got from the follow:

$$\begin{cases} N_1(\Psi) = \sum_{i=-m}^{+m}\sum_{j=-m}^{+m}\mathrm{circ}\{[x_1^2(\Psi, it, jt/\cos\Psi) + \\ y_1^2(\Psi, it, jt/\cos\Psi)]/r^2\} \\ N_0(\Psi) = \sum_{i=-m}^{+m}\sum_{j=-m}^{+m}\mathrm{circ}\left[\frac{(it)^2 + (it/\cos\Psi)^2}{r^2}\right] \end{cases} \tag{4}$$

in the function(4), x_1 and y_1 are the coordinates at which rays reach the detector, t and $t/\cos\Psi$ are the light density (light number on the unit length) on direction x and y on plane x-y, and r is the radius of the detector.

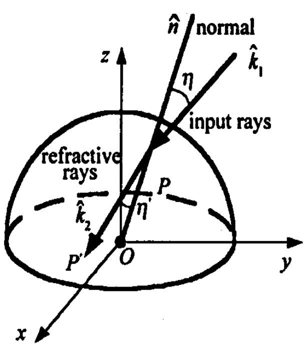

Fig. 3 The optical path of light

Fig. 3 shows the optical path of light incidence on the concentrator. The light (position vector $\hat{k}_1$) enter the hemisphere concentrator at point P, the incidence angle is η, the normal position vector of the concentrator's surface at the point P is $\hat{n}$, and the refractive angle is η. We can consider the incidence light cluster ($\hat{k}_1 = (0, \cos\Psi, \sin\Psi)$) in plane y-z or paralleling to plane y-z for the concentrator's isotropy, then we can get the light function in arbitrary plane. The light cluster's function is shown as follows:

$$y = z\tan\Psi + m_1 t/\cos\Psi,\ x = m_2 t \tag{5}$$

t is the light density on the direction x and y, $|m_i|$ $(i = 1, 2)$ $(\leqslant R/t)$ is integer.

The position vector of point P may be written $(R\cos\alpha, R\cos\beta, R\cos\gamma)$. The normal position vector $\hat{n} = (\cos\alpha, \cos\beta, \cos\gamma)$. So we can get position vector $\hat{n}$:

$$\begin{cases} \cos\alpha = \cos[\pi/2 - \arcsin(m_2 t/R)] \\ \cos\beta = \sin\alpha\left[\sin\Psi\cos\left(\arcsin\dfrac{m_1 t}{R\sin\alpha}\right) + \cos\Psi\dfrac{m_1 t}{R\sin\alpha}\right] \\ \cos\gamma = \sin\alpha\left[\cos\Psi\cos\left(\arcsin\dfrac{m_1 t}{R\sin\alpha}\right) - \sin\Psi\dfrac{m_1 t}{R\sin\alpha}\right] \end{cases} \tag{6}$$

The coordinate of point P is $R(\cos\alpha, \cos\beta, \cos\gamma)$. The position vector of incidence light $\hat{k}_1$ and refractive light $\hat{k}_2$ are respectively $(0, \cos\Psi, \sin\Psi)$ and $(\cos\alpha', \cos\beta', \cos\gamma')$ (see Fig. 3). So we can get:

$$\begin{cases} \hat{n}\cdot\hat{k}_1 = \cos\eta \\ \hat{n}\cdot\hat{k}_2 = \cos\eta' \\ \hat{k}_1\cdot\hat{k}_2 = \cos(\eta - \eta') \end{cases} \tag{7}$$

Then we can get the position vector of $\hat{k}_2$:

$$\begin{cases} \cos\alpha' = \cos\{\arcsin[\cos\alpha\sin(\eta - \eta')/\sin\eta]\} \\ \cos\beta' = \sin\alpha'\sin\{\Psi \pm \arccos[\cos(\eta - \eta')/\sin\alpha']\} \\ \cos\gamma' = \sin\alpha'\cos\{\Psi + \arccos[\cos(\eta - \eta')/\sin\alpha']\} \end{cases} \tag{8}$$

when $m_1 > 0$, "$\pm$" is "+", and when $m_1 < 0$, "$\pm$" is "−". We can get the refractive light function from the point P and position vector $\hat{k}_2$:

$$\frac{x - R\cos\alpha}{\cos\alpha'} = \frac{y - R\cos\beta}{\cos\beta'} = \frac{z - R\cos\gamma}{\cos\gamma'} \tag{9}$$

So we can get the point P' at which the refractive light enters the detector (see Fig. 3):

$$(x_1, y_1, z_1) = \left(R\cos\alpha - \frac{R\cos\gamma\cos\alpha'}{\cos\gamma'},\ R\cos\beta - \frac{R\cos\gamma\cos\beta'}{\cos\gamma'},\ 0\right) \tag{10}$$

Then we can get the gain of the hemisphere concentrator from the function (2), (4) and (10).

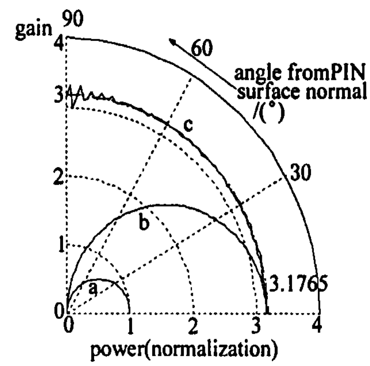

Fig. 4 Receiving power curve with concentrator, receiving power curve without concentrator, and their ratio versus incident angles, $n = 1.8$ a—unfixed concentrator b—fixed concentrator c—gain curve with angle

On the view of the final function of gain, the gain of the concentrator is the function of the incidence angle, the refractive index and the r/R. The receiving power of detector with concentrator, and without concentractor and the gain values versus the incident angles are plotted in Fig. 4 and denoted as curve a and c, which is normalized by the maximum receiving power without concentrator. As shown in Fig. 4, the gain is almost constant at different angles and is almost n^2 ($n = 1.8$). From the gain curve of Fig. 4, we can know the half FOV of the hemisphere is 90°.

The ratio of the integration of the power at different incident angles with concentrator and that without concentrator is defined as the total gain. The total gain is almost n^2 as $r/R > 1/n$, and the curves for $n = 1.3$, 1.5 and 1.78 can be observed in Fig. 5. When we choose the hemisphere concentrator, we should ensure $r/R > 1/n$ and we can get the good total gain.

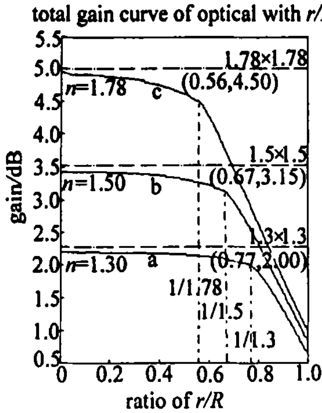

Fig. 5 Total gain curve of concentrator with r/R and n

1.2 CPC

The generatrix of CPC is a section of a parabola and a straight (see Fig. 6)[2]. As shown in Fig. 6, the incidence rays at the angle θ_1 are focused on point F_R after reflecting from paraboloid P_r, others are reflected on paraboloid S_r and exit from the concentrator at the angle θ_2, Though some of the incidence rays at angle θ_1 focus on F_R point, and the others exit from the circle surface at angle θ_2 whose diameter is F_RF_L, according to edge ray principle, the incidence rays at the angle smaller than θ_1 can exit from F_RF_L surface. The angle θ_1 is the maximum incident angle and θ_2 is the maximum exit angle. According to Eq. (1), the ideal gain is[2]:

$$C_{\text{ideal, 3dim}}(\theta_1, \theta_2) = (n\sin\theta_2/\sin\theta_1)^2 \quad (11)$$

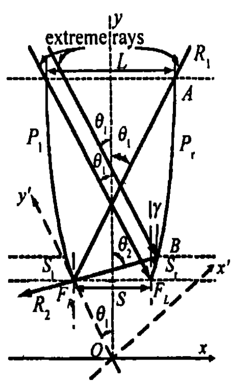

Fig. 6 Sketch of CPC

that is, FOV of CPC is θ_1. The value of ideal gain increase with n and θ_2, and decrease is with θ_1. In fact, we can get the FOV less than 90° and the gain less than $(n/\sin\theta_i)^2$.

There are several concentrators similar to CPC such as CEC (compound elliptic concentrator) and CHC (compound hyperbola concentrator), whose designs, FOV and gains are similar to those of CPC.

1.3 DTIRC

A DTIRC consists of three parts: the front surface that may be curved; the totally internally reflecting sidewall (profile); and the exit aperture. Only rays within the design acceptance angle (DTIRC's FOV) can reach the exit aperture; many rays incident on the front surface beyond the acceptance angle will finally exit from the side profile. In design, rays incident at the acceptance angle is extreme rays, and they determine the side profile of DTIRC.

Fig. 7 shows an example of a DTIRC. The extreme rays hitting the portion P_1P_2 converge into P_3', and the rays hitting the portion P_2P_3 can exit at whatever angle barely satisfies TIR (the maximum concentration method, rays is totally internally reflected on P_2P_3) or in parallel (the phase-conserving method). Now that rays incident on the front surface at the acceptance angle can exit from P_3P_3', according to edge ray principle[6, 7] the rays within the design acceptance angle also can exit from P_3P_3'.

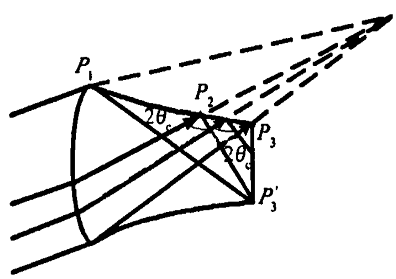

Fig. 7 Side view of a DTIRC (the maximum concentration method, rays is totally internally reflected on P_2P_3)

Fig. 8 shows the phase-conserving method. As shown in Fig. 8, typical optical path consists of four parts: l_1, l_2, l_3 and l_4. For rays converging at the bottom left-hand corner, the portion is zero. According to Fermat's principle the total optical path length is a constant for every ray connecting the initial with final wavefront. So we have the basic formula of the phase-conserving method[4]:

$$\int n\,ds = l_1 + n(l_2 + l_3 + l_4) = \text{const} \quad (12)$$

Deigning DTIRC is similar to CPC in geometry. Rays in DTIRC is totally internal reflected on the side profile observing Fermat's principle, while in CPC, rays is reflected on the side profile which is metallic or coated with the reflection coating. Thus DTIRC and

CPC are similar in shape, gain and FOV. Their gains are not very high, and their FOV are not very wide.

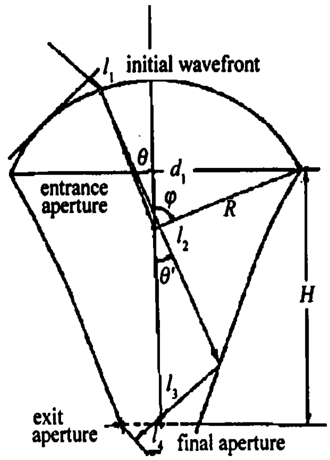

Fig. 8 Cross-section of a DTIRC(the phase-conseving method, rays exit from the exit aperture in parallel)

1.4 SMS concentrator

SMS design method appeared in the early 90's and firstly introduced the sequential mirrors and dioptrics as tools in the nonimaging optical design[8]. SMS concentrators transfer the rays emitted by the source to the receiver by means of a certain number of sequential incidences. In general, the rays suffer refraction, a metallic reflection and a totally internal reflection when they go from the source to the receiver.

In SMS design, the following symbols will be used: R= refraction, X = sequential reflection, X_F = non-sequential reflection, I_F = non-sequential total internal reflection(the subindex F means the surface coincides with a flow line)[8].

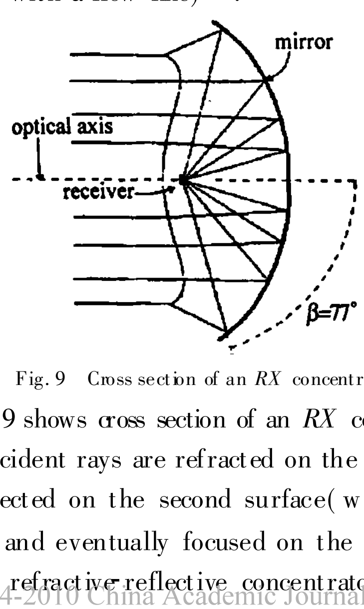

Fig. 9 Cross section of an RX concentrator

Fig. 9 shows cross section of an RX concentrator, in which incident rays are refracted on the first surface, then reflected on the second surface(with reflection coating) and eventually focused on the receiver. The device is refractive-reflective concentrator. When the refractive index is 1.5, and the acceptance angle is ±3, 95% of the maximum concentration can be achieved. The half-rim angle of illumination of the receiver is 77°, and the image-side NA = 1.46.

The SMS concentratos have high gain(able to be more than 100) and very small acceptance angle(less than one degree or several degree), the devices are suitable for LOS wireless optical communication system while not fit to diffusing wireless optical indoor communication system.

1.5 Poisson bracket concentrator

In a Poisson bracket concentrator, inhomogeneous media's refractive indexes are variable, with appropriate media and refractive index distribution rays can be merged into receiver. Poisson Bracket method[9, 10] provides the refractive index distribution and the reflector surface needed for the concentrator. There are no reflectors in Poisson Bracket concentrator and just media with variable refractive index. If the reflector is allowed, the design will be simpler.

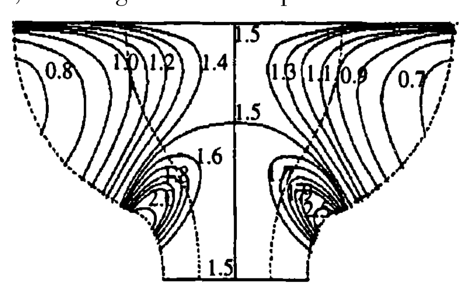

Fig. 10 Refractive-index distribution for an inhomogeneous media concentrator with acceptance angle 30° and gain 9

Fig. 10 shows the refractive-index distribution for an inhomogeneous media concentrator. Though the method is very complex and obtaining concentrator may be impractical at present because of the variable refractive index and high cost, their existence is itself important from the theoretical point of view.

1.6 Comparisons

From above, we have introduced the structures and the design methods of five nonimaging concentrators: hemispherical concentrators, CPC, DTIRC, SMS concentrator and Poisson bracket concentrator. Table 2 shows the comparison of several concentrators' FOVs and gains. In comparison, hemispherical concentrator has the widest half FOV of 90°, while its gain (n^2) is the smallest. It is suitable to hybrid

Table 2 FOVs and gains of several concentrators(n = 1.5)

concentrator	optical track	half FOV (θ_i)	gain
hemispherical concentrator	refractive	90°	2.25
CPC	refractive-reflective	less than 90°	$(n/\sin\theta_i)^2$
DTIRC	refractive-reflective	about 20°	about 20
SMS concentrator	reflective	0.75°~3°	about 114
Poisson bracket concentrator	refractive	about 30°	about 9

and non-directed wireless optical link for wide FOV. A single CPC has high gain and small FOV, and its gain is correlation to its FOV. It is fit for directed wireless optical link. A CPC combined with inverted parabolic hollow CPC can achieve FOV of 90° while reducing the gain to n^2, so its application is similar to hemispherical concentrator. DTIRC and Poisson bracket concentrator have small FOV and high gain, and they are fit for directed non-LOS link or hybrid wireless optical link(such as base-station cell communication). SMS concentrator has very high gain and very small FOV, so it is fit for directed LOS wireless optical link.

2 Conclusion

Five nonimaging concentrators are revised: hemispherical concentrator, CPC, DTIRC, SMS concentrator and Poisson bracket concentrator. Hemisphere concentrator has been analyzed in details by ray racing and the design principle is given. Then we have compared their FOV and gains, and given the application suggestion for five concentrators. Hemispherical concentrator and CPC are very fit for diffusing wireless optical indoor communication system, CPC, DTIRC and Poisson Bracket concentrator are fit for base-station cell communication system, and SMS concentrator is fit for directed LOS wireless optical communication. They are more compact and have more high gain than the imaging concentrators.

References

[1] Mohedano R, Minano J C, Benitez P. Opt Engng, 2000, 39(10): 2740~2747.
[2] Rabl A, Winston R. Appl Opt, 1976, 15(11): 2880~2883.
[3] Ho K P, Kahn J M. Opt Engng, 1995, 34(5): 1385~1395.
[4] Ning X H, Winston R, Gallaber J O. Appl Opt, 1987, 26(2): 300~305.
[5] Savicki J P, Morgan S P. Appl Opt, 1994, 33(34): 8057~8061.
[6] Davies P A. J O S A, 1994, A11(4): 1256~1264.
[7] Ries H, Rabl A. Optical Society of America, 1994, 11(10): 2627~2632.
[8] Benitez P, Mohedano R, Minano J C. SPIE, 1997, 3139: 19~28.
[9] Minano J C. Optical Society of America, 1986, 3(9): 1345~1353.
[10] Minano J C. SPIE, 1993, 2016: 98~108.